Article ID: 1003－6326(2003)02－0245－04

Preparation of low cobalt high rate discharge hydrogen storage alloy $MlNi_{3.85}Co_{0.45}Mn_{0.4}Al_{0.3}X_{0.1}$ (X= Mg, Si, Sn) ①

LIU Kai-yu(刘开宇), ZHANG Ping-min(张平民), TANG You-gen(唐有根)
(College of Chemistry and Chemical Engineering, Central South University, Changsha 410083, China)

Abstract: The non-stoichiometric high rate discharge hydrogen storage alloys series $MlNi_{3.85}Co_{0.45}Mn_{0.4}Al_{0.3}X_{0.1}$ (Ml represents the lanthanum-rich mischmetal, and X= Mg, Si, Sn) were prepared. The XRD and EDS results show that the high catalysis active miscellaneous La_2Ni_7 phase forms except for main phase $LaNi_5$ in the alloy body. The high rate discharge performance of hydrogen storage alloys electrode was improved because of the formation of La_2Ni_7 phase. The discharge capacities at 0.2C, 1C and 5C discharge rate reach 320 mAh·g^{-1}, 300 mAh·g^{-1} and 260 mAh·g^{-1} respectively when X is (Mg+ Si). At the same scanning rate of circular volt—ampere testing, the surface anode oxidation peak current and peak area of the alloy containing (Mg+ Si) electrode are far more larger than that of the high cobalt alloy $MlNi_{3.55}Co_{0.75}Mn_{0.4}Al_{0.3}$ (AB_5). Furthermore, the cobalt content of the hydrogen storage alloy containing (Mg+ Si) decreases by 40% and the high rate discharge performance improves obviously compare to high cobalt AB_5 alloys, it is promising that the hydrogen storage alloy containing (Mg+ Si) becomes to an ideal dynamic battery cathode material.

Key words: low cobalt; high rate discharge; hydrogen storage alloys; (Mg+ Si); preparation
CLC number: TE 139$^+$.7 **Document code:** A

1 INTRODUCTION

In recent years, Ni/MH battery that is a new generation battery with high energy density was rapidly developed afterwards Ni/Cd battery. With the increasingly mature of Ni/MH battery production technique, it begins to join the field of high power and great capacity cell, and becomes gradually the most promising green dynamic cell that was applied to electromotive motor. The hydrogen storage alloy, as the key material of Ni/MH dynamic cell, must be characterized by its high special capacity, high voltage platform, good catalyze activity, long cycle life and lower cost[1-3]. A lot of study have been fulfilled by researchers inside and outside in order to improve the performance index[4-8]. In this paper, the dynamic type hydrogen storage alloy was prepared with a view to the accession of microelement and non-stoichiometric method.

2 EXPERIMENTAL

2.1 Preparation of hydrogen storage alloy powder

Raw materials: lanthanum rich mischmetal Ml (La/Re ≥99.5%), lanthanum-neodymium alloy (La 52.49%, Ce 4.41%, Pr 5.10%, Nd 37.38%) and rich cerium alloy (La 27.51%, Ce 51.93%, Pr 5.06%, Nd 15.37%) were mixed to be the experimental commix rare earth according to a certain proportion; the simple substance purity is Ni 99.95%, Co 99.97%, Mn 99.8%, Al 99.7%, Mg 99.5%, Si 99.5% and Sn 99.99% respectively.

Preparation of hydrogen storage alloy powder: according to the designed proportion, the alloy ingot was obtained in 25 kg level intermediate frequency induction furnace in argon atmosphere, the hydrogen storage alloy powder whose granularity is less than 106 μm was obtained via anneal, punch milling at liquid medium, dryness techniques.

2.2 Preparation of single electrode and simulation cell

The hydrogen storage alloy powder and nickel powder were equably mixed at the proportion of 2∶1, according to quantitative PTFE latex of 1% concentration, after drying in vacuum, a hydrogen storage alloy electrode of 11 mm in diameter was compacted on a pressing machine at pressure of 4 MPa. As the simulation cell, the positive pole is a big superficial sintering nickel, the negative pole is hydrogen storage alloy electrode, the electrolyte is 6 mol·L^{-1} KOH solution. Cell order-control testing apparatus fulfilled the electrochemistry capacity and cycle stability performance, the testing condition is:

1) 0.2C charge under constant current for 4 h, rest for 5 min, 0.2C discharge under constant current up to the cell end voltage reaches 1.05 V;

① **Foundation item:** Project (2001AA501433) supported by the National High Technology R&D Program of China
Received date: 2002－04－12; **Accepted date:** 2002－09－19
Correspondence: Dr. LIU Kai-yu, Tel: +86-731-8830886; E-mail: kaiyuliu@263.net

0.2C charge under constant current for 6 h, rest for 5 min, 0.2C discharge under constant current up to the cell end voltage reaches 1.00 V; 0.2C charge under constant current for 6 h, rest for 5 min, 0.2C discharge under constant current up to the cell end voltage reaches 1.00 V.

2) 1C charge under constant current for 72 min, rest for 5 min, 1C discharge under constant current up to the cell end voltage reaches 1.00 V, cycle 5 times.

3) 1C charge under constant current for 72 min, rest for 5 min, 5C discharge under constant current up to the cell end voltage reaches 0.90 V, cycle 5 times.

For above mentioned 1), 2) and 3), the last discharge capacities are respectively regarded to the 0.2C, 1C and 5C electrochemistry capacity of alloy electrode.

4) The cycle stability performance testing condition: 3C charge under constant current for 25 min, rest for 5 min, 3C discharge under constant current up to the cell end voltage reaches 0.95 V, cycle. Until the discharge capacity decreases 70% of initial stable discharge capacity, its life ends.

The cycle volt—ampere testing was carried out in three-electrode system, the positive pole is a big superficial sintering nickel, the negative pole is the experimental hydrogen storage alloy electrode, reference electrode is Hg/HgO (6 mol·L^{-1} KOH), the electrolyte is 6 mol·L^{-1} KOH solution, scanning potential range is from −0.30V to −1.30 V (vs Hg/HgO).

2.3 Material structure and component analyses

The X-ray diffraction is carried out on the Japanese-made D/max-rA, Cu target, tube voltage is 36 kV, working current is 30 mA. The hexad-side lattice constants was gained by means of the imitation of five diffraction peak of (101), (110), (200), (111) and (201) within 25°−50° degree of 2θ using the least quadric multiplication method.

EDS fulfilled the observation of alloy structure and the analyses of alloy chemistry component.

3 RESULTS AND DISCUSSION

3.1 Microstructure analyses

Fig. 1 is the phase diagram of $LaNi_5$ type hydrogen storage alloy[9], which shows that the phase should be AB_5 and AB_4 when the liquid state alloy M was slowly cooled down from 1 500 ℃ to room temperature (approximately balance process). In practically, it is impossible that the P_1 bundle crystal reaction (reaction 1) can ideally be performed under 995 ℃ because of the rapidly dropping temperature of liquid state alloy, so, the P_2 and P_3 bundle crystal

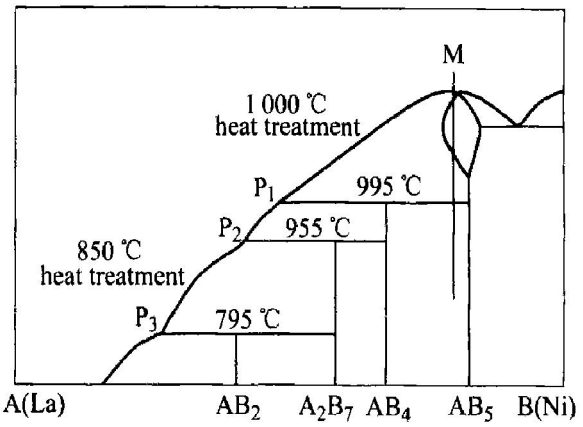

Fig. 1 Phase diagram of $LaNi_5$ type hydrogen storage alloy

reaction (reaction 2 and 3) will then take place:

$$L_{P_1} + S_{AB_5} \rightarrow S_{AB_4} \quad (995\ ℃) \quad (1)$$

$$L_{P_2} + S_{AB_4} \rightarrow S_{A_2B_7} \quad (955\ ℃) \quad (2)$$

$$L_{P_3} + S_{A_2B_7} \rightarrow S_{AB_2} \quad (795\ ℃) \quad (3)$$

As a result, the agglomerating state structure of casting alloy is constituted by the matrix phase AB_5 and the secondary phase AB_4, A_2B_7, AB_2. When the heat treatment is carried out under 1 000 ℃, reaction 1 acts conversely, it is in favor of the transformation from secondary phase AB_4 to matrix phase AB_5. When the heat treatment is carried out at 850 ℃, the reaction $S_{AB_2} \rightarrow L_{P_3} + S_{A_2B_7}$ and $L_{P_2} + S_{AB_4} \rightarrow S_{A_2B_7}$ will happen, it is beneficial to the forming of A_2B_7 phase.

Fig. 2 is the XRD pattern of $MlNi_{3.85}Co_{0.45}Mn_{0.4}Al_{0.3}(Mg+Si)_{0.1}$ after heat treatment, it is clear that the alloy secondary phase almost disappeared after 1 000 − 850 ℃ two-step heat treatment, the treated alloy is composed of matrix phase AB_5 and secondary phase A_2B_7.

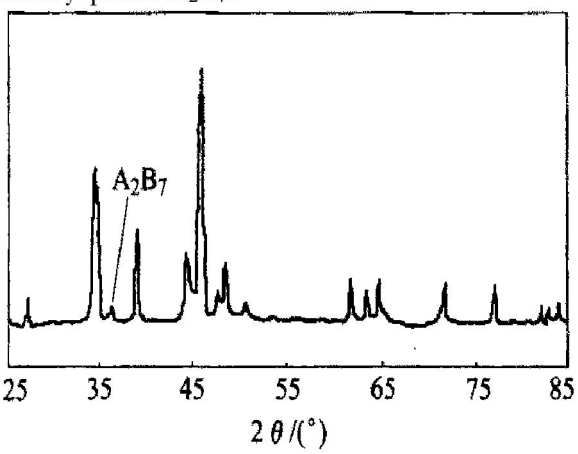

Fig. 2 XRD pattern of $MlNi_{3.85}Co_{0.45}Mn_{0.4}Al_{0.3}(Mg+Si)_{0.1}$ after heat treatment

The X-ray diffraction results show that the structure of $MlNi_{3.85}Co_{0.45}Mn_{0.4}Al_{0.3}X_{0.1}$ (X= Mg, Si, Sn) is $CaCu_5$ type, there is secondary phase A_2B_7 peak besides the matrix phase AB_5 peak. Combined

with the results of EDS analyses (Table 1), the structure of "matrix phase+ secondary phase" can be discovered. In the charge and discharge processing, the electrode can form the comparatively instability hydride phase and the catalyze activity can be improved, the absorb-expend hydrogen dynamic performance can be modified because of the forming of secondary phase[10].

Table 2 lists the lattice constants of the experimental alloy. It shows that the lattice volume of alloys containing Mg, Si, Sn and (Mg+ Si) is appreciably smaller than that of the alloy with high cobalt AB_5 type, the ratio of c_0/a_0 is very approach.

Table 1 Results of EDS analyses for phases (mole fraction, %)

Phase	Re	Ni	Co	Mn	Al	Mg+ Si	Phase
Matrix phase	19.2	69.8	4.2	5.1	1.2	0.5	AB_5
Secondary phase	22.3	66.7	4.0	4.9	1.3	0.8	A_2B_7

Table 2 Lattice constants of $MlNi_{3.85}Co_{0.45}Mn_{0.4}Al_{0.3}X_{0.1}$ and AB_5 alloys

Alloy	a_0/ nm	c_0/ nm	c_0/a_0	V/ nm^3
AB_5	0.502 0	0.402 9	0.801	0.089 1
$MlNi_{3.85}Co_{0.45}Mn_{0.4}Al_{0.3}Mg_{0.1}$	0.502 2	0.401 0	0.798	0.087 5
$MlNi_{3.85}Co_{0.45}Mn_{0.4}Al_{0.3}Si_{0.1}$	0.502 8	0.402 7	0.801	0.088 9
$MlNi_{3.85}Co_{0.45}Mn_{0.4}Al_{0.3}Sn_{0.1}$	0.502 0	0.400 5	0.798	0.087 2
$MlNi_{3.85}Co_{0.45}Mn_{0.4}Al_{0.3}(Mg+Si)_{0.1}$	0.502 4	0.401 8	0.799	0.088 0

Table 3 lists the lattice constants of the experimental alloy after absorbing hydrogen, illuminating that the lattice volume of the absorbed hydrogen alloy increases in some degree, and the expending ratios of lattice volume of alloys containing (Mg+ Si) and Sn reach 18.53% and 19.32%, it is close to that of the high cobalt AB_5 type alloy 17.63%, however, the expending ratios of lattice volume of alloys containing Mg or Si only increase distinctly compared to high cobalt AB_5 type alloy, reaching 21.88% and 20.35% respectively. The expending ratio of alloy will give rise to the cycle stability of hydrogen storage electrode, therefore, the addition of (Mg+ Si) or Sn can decrease the expending of lattice volume of alloys after absorbing hydrogen, it can not only improve alloy resistance ability of pulverization, but also reduce the cobalt content of alloy to 60% compared to the high cobalt AB_5 type alloy (from 0.75 mol to 0.45 mol).

Table 3 Lattice constants of $MlNi_{3.85}Co_{0.45}Mn_{0.4}Al_{0.3}X_{0.1}$ and AB_5 alloys after absorbing hydrogen

Alloy	a_0/ nm	c_0/ nm	c_0/a_0	V/ nm^3	ΔV/ V
AB_5	0.537 4	0.418 9	0.779	0.104 8	17.63%
$MlNi_{3.85}Co_{0.45}Mn_{0.4}Al_{0.3}Mg_{0.1}$	0.547 3	0.417 7	0.763	0.106 6	21.88%
$MlNi_{3.85}Co_{0.45}Mn_{0.4}Al_{0.3}Si_{0.1}$	0.540 1	0.418 9	0.776	0.107 0	20.35%
$MlNi_{3.85}Co_{0.45}Mn_{0.4}Al_{0.3}Sn_{0.1}$	0.542 1	0.416 6	0.768	0.104 0	19.32%
$MlNi_{3.85}Co_{0.45}Mn_{0.4}Al_{0.3}(Mg+Si)_{0.1}$	0.540 9	0.415 7	0.769	0.104 3	18.53%

3.2 Results of cyclic volt—ampere

The electrode cycle volt-ampere results of the high cobalt AB_5 type alloy and low cobalt alloy containing (Mg+ Si) are shown in Table 4. At the same scanning rate, the anode oxidation peak current and peak area of hydrogen on (Mg + Si) alloy electrode surface is far more greater than that of the high cobalt AB_5 type alloy electrode, which indicates that the addition of (Mg+ Si) to cobalt can distinctly improve the discharge capacity and surface catalyze activity of hydrogen storage alloy electrode. The larger the scanning rate of the same electrode, the less the anode peak electricity quantity, which indicates that the release of hydrogen in alloy is restricted along with the increase of scanning rate. The anode peak current of electrode can be increased and the surface electrochemistry reaction activity of electrode can be improved by adding (Mg+ Si) to cobalt and non-stoichiometric method. The increase of surface catalyze activity and electrochemistry reaction activity of electrode guarantees the high rate discharge performance of hydrogen storage electrode.

Table 4 Circular volt—ampere characteristics of MH electrode

Electrode	Scanning velocity /(mV·s^{-1})	Anodic peak capacity Q/ C	Anodic peak current J_P/ mA
AB_5	100	1.80	311
	64	2.14	218
	36	2.53	167
	16	3.25	104
	9	4.57	69
$MlNi_{3.85}Co_{0.45}Mn_{0.4}Al_{0.3}(Mg+Si)_{0.1}$	100	6.53	133 5
	64	7.44	109 8
	36	9.26	712
	16	14.17	431
	9	19.88	309

3.3 Electrochemistry properties

The results of discharge special capacity at different discharge ratios, high rate discharge characteristics and cycle stability properties of hydrogen storage alloy electrode are listed in Table 5. The partial replacement of Mg, Si, Sn and (Mg+ Si) to cobalt in alloy can certainly improve the high rate discharge characteristics. By the way, although the cycle stability properties of alloy electrode decrease distinctly while only adding Mg or Si, which is identical with Refs. [11, 12], the cycle stability properties of the addition of (Mg + Si) alloy are very close to the high cobalt AB_5 type alloy. The affecting mechanism is not entirely clear at present, however, the experimental results illustrate that not only the cycle stabilities can not be affected, but also the electrochemistry capacity and high rate discharge characteristics can be improved and the product cost of hydrogen storage alloy can distinctly be decreased if the cobalt is in reason replaced by (Mg+ Si).

Table 5 Discharge special capacity, high rate characteristics and cycle stability properties of hydrogen storage alloy electrode

Alloy	Discharge capacity/ (mAh·g^{-1})			HRD*	Cycle life
	0.2C	1C	5C		
AB_5	317	290	226	0.713	450
$MlNi_{3.85}Co_{0.45}Mn_{0.4}Al_{0.3}Mg_{0.1}$	309	281	235	0.761	328
$MlNi_{3.85}Co_{0.45}Mn_{0.4}Al_{0.3}Si_{0.1}$	311	288	227	0.730	394
$MlNi_{3.85}Co_{0.45}Mn_{0.4}Al_{0.3}Sn_{0.1}$	303	291	242	0.799	404
$MlNi_{3.85}Co_{0.45}Mn_{0.4}Al_{0.3}(Mg+Si)_{0.1}$	322	302	268	0.832	436

* $HRD = C_{5C}/C_{0.2C}$

4 CONCLUSIONS

1) In the charge and discharge processing, the electrode can form the comparatively instability hydride phase, the catalyze activity can be improved, the absorb-expend hydrogen dynamic performance can be modified, because of the formation of secondary phase A_2B_7.

2) At the same scanning rate, the anode oxidation peak current and peak area of hydrogen on (Mg+ Si) alloy electrode surface are far more greater than those of the high cobalt AB_5 type alloy electrode, the addition of (Mg+ Si) to cobalt can distinctly improve the discharge capacity and surface catalyze activity of hydrogen storage alloy electrode.

3) The partial replacement of Mg, Si, Sn and (Mg+ Si) to cobalt in alloy can certainly improve the high rate discharge characteristics.

REFERENCES

[1] WU Bo-rong. The MH-Ni dynamic battery using for electromotive vehicle [J]. Chinese Journal of Power Source, 2000, 24(1): 45-48. (in Chinese)

[2] Lichenberg F, Kohler U, Foler A, et al. Development of AB_5 type hydrogen storage alloys with low Co content for rechargeable Ni-MH batteries with respect to electric vehicle applications[J]. J Alloys Comps, 1997, 253-254 (8): 570-573.

[3] REN Ke, LEI Yong-quan, CHEN Li-xin, et al. Phase structures and hydrogen storage capabilities of the alloys $Ml_x(Ni_{3.8}Co_{0.75}Mn_{0.4}Ti_{0.05})$ [J]. Rare Metal Materials and Engineering, 2000, 29(4): 235-238. (in Chinese)

[4] JIANG Jian-jun, LEI Yong-quan, SUN Da-lin, et al. Mechanism of La, Ce, Pr and Nd on the electrochemical properties of multi-components $RE(NiCoMnAl)_5$ hydrogen storage alloys [J]. Journal of the Chinese Rare Earth Society, 1997, 15(4): 318-324. (in Chinese)

[5] Suzuki T, Yanagihara M, Kawana H, et al. Effect of rare earth composition on the electrochemical properties of $Mm(NiCoMnAl)_5$ alloys [J]. J Alloys and Comp, 1993, 192(11): 173-182.

[6] Ewe H H. Electrochemical accumulation and oxidation of hydrogen using the intermetallic compound lanthanum-nickel($LaNi_5$) [J]. Energy Converse, 1973, 13(7): 109-118.

[7] Adzic G D, Johnson J R. Cerium content and cycle life of multi-composition AB_5 hydride electrodes [J]. J ElectroChem Soc, 1995, 142(10): 342-349.

[8] WANG Zhi-xing, LI Xin-hai. Structure of Sn doped AB_5 non-stoichiometric hydrogen absorbing alloys[J]. Journal of the Chinese Rare Earth Society, 2000, 18(2): 128-131. (in Chinese)

[9] XU Guang-xian. Rare Earth, 2rd ed [M]. Beijing: Metallurgical Industry Press, 1995. 288. (in Chinese)

[10] CHEN Wei-xiang. Study of circular volt—ampere and AC impedance of hydrogen storage alloy electrode [J]. Chinese Journal of Power Sources, 2000, 24(4): 200-203. (in Chinese)

[11] CHEN Li-xin. Effects of Mg doping on electrochemical properties of $Ml(NiCoMnTi)_5$ hydrogen storage electrode alloy [J]. The Chinese Journal of Nonferrous Metals, 1999, 9(1): 61-64. (in Chinese)

[12] CHEN Li-xin, LEI Yong-quan. Effects of Si doping on electrochemical properties of $Ml(NiCoMnTi)_5$ hydrogen storage electrode alloy [J]. Nonferrous Metals, 1998, 50(2): 104-107. (in Chinese)

(Edited by HUANG Jin-song)